

COMPONENT PART NOTICE

THIS PAPER IS A COMPONENT PART OF THE FOLLOWING COMPILATION REPORT: **A**

(TITLE): Characteristics of the Lower Atmosphere Influencing Radio Wave Propagation:
Conference Proceedings of the Symposium of the Electromagnetic Wave
Propagation Panel (33rd) Held at Spatind, Norway on 4-7 October 1983.

(SOURCE): Advisory Group for Aerospace Research and Development, Neuilly-sur-Seine
(France).

TO ORDER THE COMPLETE COMPILATION REPORT USE AD-A145 046.

THE COMPONENT PART IS PROVIDED HERE TO ALLOW USERS ACCESS TO INDIVIDUALLY AUTHORED SECTIONS OF PROCEEDINGS, ANNALS, SYMPOSIA, ETC. HOWEVER, THE COMPONENT SHOULD BE CONSIDERED WITHIN THE CONTEXT OF THE OVERALL COMPILATION REPORT AND NOT AS A STAND-ALONE TECHNICAL REPORT.

THE FOLLOWING COMPONENT PART NUMBERS COMPRISE THE COMPILATION REPORT:

AD#:	TITLE:
AD-P003 885	Ice Depolarization on Low-Angle 11 GHz Satellite Downlinks.
AD-P003 886	The Effects of a Low-Altitude Nuclear Burst on Millimeter Wave Propagation.
AD-P003 887	Measurements of Atmospheric Effects on Satellite Links at Very Low Elevation Angle.
AD-P003 888	The Effects of Meteorology on Marine Aerosol and Optical and IR Propagation.
AD-P003 889	A System to Measure LOS (Line-of-Sight) Atmospheric Transmittance at 19 GHz.
AD-P003 890	A GaAs FET Microwave Refractometer for Tropospheric Studies.
AD-P003 891	Prediction of Multipath Fading on Terrestrial Microwave Links at Frequencies of 11 GHz and Greater.
AD-P003 892	Multipath Outage Performance of Digital Radio Receivers Using Finite-Tap Adaptive Equalizers.
AD-P003 893	Spherical Propagation Models for Multipath-Propagation Predictions.
AD-P003 894	Correcting Radio Astronomy interferometry Observations for Ionospheric Refraction.
AD-P003 895	The Estimation and Correction of Refractive Bending in the AR3-D Tactical Radar Systems.
AD-P003 896	Effect of Multiple Scattering on the Propagation of Light Beams in Dense Nonhomogeneous Media.
AD-P003 897	Adaptive Compensation for Atmospheric Turbulence Effects on Optival Propagation.
AD-P003 898	Effects of Atmospheric Turbulence on Optical Propagation.
AD-P003 899	A Radio Interference Model for Western Europe.
AD-P003 900	Transhorizon Microwave Propagation Measurements related to Surface Meteorological Parameters.
AD-P003 901	Tropospheric Propagation Assessment.

COMPONENT PART NOTICE (CON'T)

AD#:	TITLE:
AD-P003 902	Distortion of a Narrow Radio Beam in a Convective Medium.
AD-P003 903	Anomalous Propagation and Radar Coverage through Inhomogeneous Atmospheres.
AD-P003 904	The Prediction of Field Strength in the Frequency Range 30 - 1000 MHz.
AD-P003 905	VHF and UHF Propagation in the Canadian High Arctic.
AD-P003 906	Considerations Pertinent to Propagation Prediction Methods Applied to Airborne Microwave Equipments.

Accession For	
NTIS GRA&I	<input checked="" type="checkbox"/>
DTIC TAB	<input type="checkbox"/>
Unannounced	<input type="checkbox"/>
Justification	
By _____	
Distribution/	
Availability Codes	
Dist	Avail and/or Special
A-1	

THE EFFECTS OF A LOW-ALTITUDE
NUCLEAR BURST ON MILLIMETER
WAVE PROPAGATION

by
Edward E. Altshuler
Rome Air Development Center
Electromagnetic Sciences Division
Hanscom AFB, MA 01731
U.S.A.

SUMMARY

The main objective of this paper is to examine the limitations imposed on millimeter wave propagation by the dust produced by a low altitude nuclear burst. The closer the burst is to the surface, the larger will be the dust loaded into the nuclear fireball, an extremely hot and highly ionized spherical mass of air and gaseous weapon residues. The fireball absorbs, scatters and refracts the propagated wave and may also produce scintillations. In this study, only losses due to absorption and scattering are calculated.

Since there is a great deal of uncertainty as to how representative the dust model is of the true nuclear environment, a sensitivity analysis of attenuation dependence on the pertinent dust parameters was first conducted. It was found that the dust attenuation is very heavily dependent on the maximum particle radius, the number of large particles in the distribution and the real and imaginary components of the index of refraction over the range from dry sand to clay. The attenuation is also proportional to the fraction of the atmosphere filled with dust. The total attenuation produced by a 1 megaton burst at the surface is then computed using the WESCOM code. The attenuation includes losses due to fireball ionization, dust and atmospheric oxygen and water vapor. Results are obtained as a function of time after burst, distance from burst, elevation angle and frequency up to 95 GHz. It is found that very high attenuations occur within about 20 seconds after the burst if the path intersects the fireball. At later times attenuations of the order of tens of dB are possible due to dust alone. After several minutes the larger dust particles have settled and attenuations of several dB are present. Oxygen and water vapor attenuations are typically less than one dB in the window regions.

1. INTRODUCTION

In this paper the limitations imposed on millimeter waves by a low altitude nuclear burst are examined. Associated with the burst is a fireball, an extremely hot and highly ionized spherical mass of air and gaseous weapon residues. The fireball grows rapidly and because of its intense heat some of the soil and other material in the area are vaporized and taken into the fireball; strong afterwinds cause large amounts of dirt and debris to be sucked up as the fireball rises.

In order to estimate the effects of dust on the performance of a millimeter wave system it is necessary to first develop a dust model. Since there is a great deal of uncertainty as to how representative the model is of the true nuclear environment, a sensitivity analysis of the attenuation dependence on pertinent dust parameters is conducted. It is assumed that the dust particle sizes follow a power law distribution. Then the attenuation is computed as a function of minimum particle radius, maximum particle radius, particle size distribution, index of refraction and density. A Mie formulation is used to calculate the absorption and scattering losses produced by dust.

The total attenuation produced by a 1 Megaton surface burst is then computed using the WESCOM code. The attenuation consists of contributions due to fireball ionization, dust and atmospheric oxygen and water vapor. Attenuations are obtained as a function of time after burst, distance from burst, elevation angle and frequency.

2. PARTICLE SIZE DISTRIBUTION

The sizes of dust particles are often represented by a power law probability distribution of the form

$$P(r) = kr^{-p} \quad (1)$$

where r is the particle radius, p is the exponent and k is a constant, selected such that $P(r)$ is a proper probability distribution. For some applications a log-normal distribution of particle sizes is used since it provides a better model of the very small particles. For this study, however, we will show that the actual distribution of the very small dust particles does not significantly affect the attenuation so the power law distribution is suitable.

Thus

$$k \int_{r_{\min}}^{r_{\max}} r^{-p} dr = 1 \quad (2)$$

Solving for k we have

$$k = \frac{p-1}{r_{\min}^{-(p-1)} - r_{\max}^{-(p-1)}} \quad (3)$$

where r_{\min} and r_{\max} are the minimum and maximum particle radii respectively. The total number of particles of radius r is then

$$N(r) = N_T P(r) \quad (4)$$

where N_T is the total number of dust particles,

$$N_T = \frac{M_T}{\rho_b \bar{V}} \quad (5)$$

and

$$\begin{aligned} M_T &= \text{total mass of particulates} \\ \rho_b &= \text{bulk density of particulate material} \\ \bar{V} &= \text{mean volume of a particulate} \end{aligned}$$

Then

$$N(r) = \frac{M_T}{\rho_b (4/3 \pi r^3)} \cdot \frac{r^{p-1}}{r_{\min}^{-(p-1)} - r_{\max}^{-(p-1)}} r^{-p} \quad (6)$$

It can be shown that

$$\frac{1}{r^3} = \frac{p-1}{p-4} \cdot \frac{r^{-(p-4)}_{\min} - r^{-(p-4)}_{\max}}{r^{-(p-1)}_{\min} - r^{-(p-1)}_{\max}} \quad (7)$$

Finally

$$N(r) = \frac{M_T (p-4) r^{-p}}{4/3 \pi \rho_b \left[r^{-(p-4)}_{\min} - r^{-(p-4)}_{\max} \right]} \quad (8)$$

3. ATTENUATION OF DUST PARTICLES

Millimeter waves incident on atmospheric particulates undergo absorption and scattering, the degree of each being dependent on the size, shape and complex dielectric constant of the particle and the wavelength and polarization of the wave. An expression for calculating the absorption and scattering from a dielectric sphere was first derived by Mie (1908). It has the form

$$Q_t = -\frac{\lambda^2}{2\pi} \operatorname{Re} \sum_{n=1}^{\infty} (2n+1) (a_n^s + b_n^s) \quad (9)$$

where Q_t , the extinction cross section, represents losses due to both absorption Q_a , and scattering Q_s , and a_n^s and b_n^s are very complicated functions of the spherical Bessel terms that correspond to the magnetic and electric modes of the particle respectively. Q_t has the dimension of area and is usually expressed as cm^2 . Physically, if a wave having a flux density of S watts/ cm^2 is incident on the particle, then $S \times Q_t$ is the power absorbed and scattered.

When the size of a dust particle is very small with respect to wavelength, then the Rayleigh approximation is valid. For this case

$$Q_a = \frac{8\pi^2 r^3}{\lambda} \operatorname{Im} \left(-\frac{n^2-1}{n^2+2} \right) \quad (10)$$

$$Q_s = \frac{128\pi^5 r^6}{3\lambda^4} \left| \frac{n^2-1}{n^2+2} \right|^2 \quad (11)$$

It is seen that the absorption is inversely proportional to the wavelength while the scattering loss is inversely proportional to the fourth power of the wavelength; thus when the wavelength is large compared to the particle size, the absorption dominates and scattering losses are often assumed negligible. Furthermore, since the absorption is proportional to the particle volume, the total attenuation is proportional to the total volume of dust.

As the dust particles become larger, then the Rayleigh approximation is no longer valid and the Mie formulation must be used. Both absorption and scattering cross sections continue to increase with particle size. Finally, after reaching a peak the total cross section begins to level off and would eventually approach a value of twice the geometric cross section of the particle when it is very large with respect to wavelength (Van de Hulst, 1957). Thus we note that as the particle becomes larger the extinction cross section which was initially proportional to the particle volume becomes proportional to the particle cross sectional area.

The attenuation coefficient is equal to

$$\alpha = \int_0^{\infty} N(r) Q_t dr \quad (12)$$

This expression is in nepers/cm, if r and Q_t have units of cm and $N(r)$ is in cm^{-3} . In order to convert to dB/km a multiplicative factor of 4.343×10^3 must be introduced.

Attenuation and albedo, the ratio of scattered loss to total loss $\frac{Q_s}{Q_t}$, for a particle size power law distribution are plotted in Fig. 1 for sand and clay for frequencies from 10 to 95 GHz. It is assumed that the minimum and maximum particle radii are .005 and 5 mm respectively, that the power law exponent is -3.5, and that the densities of the dust material and average mass are 2.6 gm/cm^3 and 100 gm/m^3 respectively. It is seen that the attenuation increases very rapidly with increasing frequency. It should be pointed out that attenuation is plotted on a logarithmic scale so the apparent linear increase in attenuation at the higher frequencies actually corresponds to an exponential increase, in reality. Since clay has a higher index refraction than sand, the attenuations are significantly higher.

The ratio of the scattering losses to the total losses, often referred to as the albedo, is also plotted in Fig. 1. It is interesting to note that the albedo for sand is approximately .7, even for a wavelength as long as 30 mm when the average particle radius is only .02675 mm, less than .001 wavelength. This indicates that even though the average dust particles are very small with respect to wavelength the scattering losses are certainly not negligible as compared to the absorption because of the limited number of large particles that are present. This issue is discussed later when the results of the albedo dependence on maximum particle radius are presented.

3A. Dependence of Dust Attenuation on Minimum Particle Radius

In Figs. 2(a) and 2(b) the attenuations are plotted for sand and clay respectively as a function of minimum particle radius for a set of frequencies from 10 to 95 GHz. It is seen that the attenuation rises only very slightly as the minimum particle radius is increased. It is interesting to note that it passes through a very broad peak at 95 GHz and would probably behave similarly at the lower frequencies for larger minimum particle radii. On the basis of these results it can be concluded that the attenuation is not very sensitive to the minimum particle radius.

3B. Dependence of Dust Attenuation and Albedo on Maximum Particle Radius.

In Figs. 3(a) and 3(b) the attenuations and albedos are plotted for sand and clay respectively as a function of maximum particle radius for the same set of frequencies from 10 to 95 GHz. It is seen that the attenuation and albedo both rise very abruptly as the maximum particle radius is increased. The attenuation reaches a peak and the albedo begins to level off when the maximum particle diameter is approximately equal to the wavelength. As mentioned previously it is seen that the scattering losses are comparable and in some instances even larger than the absorption losses. This is due to the fact that the imaginary component of the index of refraction is very small, thus resulting in a small absorption.

3C. Dependence of Dust Attenuation on the Power Law Exponent

In Figs. 4(a) and 4(b) attenuation is plotted as a function of power law exponent for sand and clay respectively for the set of frequencies from 10 to 95 GHz. When the exponent p , is small the probability of having large particles in the distribution is relatively high. As p becomes larger fewer large particles are present. Thus the attenuation passes through a very broad peak for low values of p and then drops off very rapidly when p becomes larger. Thus the power law exponent can significantly affect the attenuation.

3D. Dependence of Dust Attenuation and Albedo on the Index of Refraction

In Fig. 5 the attenuation and albedo are plotted as a function of index of refraction $n = n_1 - jn_2$, for the set of frequencies from 10 to 95 GHz. Both the real and imaginary components of the index of refraction are increased linearly so that the particulates have an index of refraction that corresponds to dry sand for the lowest values and water for the highest values. It is seen that the attenuation increases and the albedo decreases sharply as the particulates change from dry sand to clay and then both essentially level off as the real and imaginary components are increased further. The attenuation and albedo are examined more closely in Fig. 6. In Fig. 6(a) the imaginary component is fixed at $n_2 = .2$ and the real component is varied from 1.6 to 3.4; in Fig. 6(b) the real component is fixed at $n_1 = 2.5$, and the imaginary component is varied from zero to .6. For both cases the attenuation increases gradually as either of the components of index of refraction is increased. Based on the curves for the albedo it is seen that increasing the imaginary component, increases the absorptive losses while increasing the real component results in an increase in the scattering losses. Thus it can be concluded that the attenuation is very dependent on both the real and imaginary components of the index of refraction over the ranges from about $2 < n_1 < 4$ and $0 < n_2 < .8$.

3E. Dependence of Dust Attenuation on Density of Particles

In Eq. (5) it is seen that the total number of dust particles is directly proportional to the total mass of the particles M_T , divided by the bulk density ρ_b of the individual particles. In this formulation a single scattering model is used so the attenuation is directly proportional to the number of particles as seen in Eq. (12) and therefore directly proportional to M_T/ρ_b . Thus any uncertainty in either the total mass or particle density will produce a corresponding error in the attenuation.

4. ATTENUATION PRODUCED BY A NUCLEAR BURST

As mentioned previously associated with the nuclear burst is a fireball. The initial electron density within the fireball is extremely high and for a period of about 20 seconds blacks out the propagated wave. After that time, beta radiation from the radioactive debris within the fireball may sustain sufficiently high ionization levels to absorb millimeter wave signals for several minutes. Thus the two principal sources that attenuate the propagated wave are fireball ionization and dust.

The nuclear explosion dust model is often divided into five distinct regions which are modeled somewhat crudely in Fig. 7. The ejecta region consists of relatively large particles of dust and debris thrown out of the crater; settling occurs quickly and its importance diminishes in about a minute or so. The blast wave produces a low level dust region often referred to as the pedestal or sweep-up layer. This region has high dust densities for about a minute also; lower densities exist for many minutes later. The cylindrical stem region forms after the establishment of the fireball vortex and lasts for several minutes. The mushroom shaped cloud or main cloud is the major dust region and exists for many minutes. Finally, the main cloud transcends into the fallout region which exists for a long period of time.

In this study the Weapons Effects on Satellite Communications code (WESCOM) is used. It utilizes environment, propagation and signal processing models developed by the Defense Nuclear Agency (DNA) and attempts to provide a best estimate of the quantities being modeled. Included along with ionization and dust losses are the oxygen and water vapor losses of the ambient troposphere.

The WESCOM dust model is a somewhat simplified model in that it assumes that all the dust is initially contained within the fireball and then forms a main cloud which eventually becomes the fallout region (Thompson, 1978). The stem and pedestal are not included in the WESCOM dust model. Dust particles within the fireball are divided into the 8 particle size ranges shown in Table 1. Each group of particle sizes are initially assumed to be uniformly distributed throughout a disc-like cylinder.

TABLE 1. Particle Size Distribution

DUST GROUP	MINIMUM PARTICLE DIAMETER	FRACTION OF PARTICLES
1	.01 mm	$1-1.372 \times 10^{-6}$
2	.9	1.356×10^{-6}
3	4.0	1.463×10^{-8}
4	10.0	8.750×10^{-10}
5	20.0	9.587×10^{-11}
6	32.5	2.222×10^{-11}
7	52.5	4.540×10^{-12}
8	75	1.370×10^{-12}

These discs are stacked within the fireball as shown in Fig. 8(a) with the largest particles contained within the lowest disc and with decreasingly smaller particles in the upper discs. Each particle size group rises to a maximum altitude at which point the particles start to fall with their respective terminal velocities. A simplified model of the size and height of the rising fireball as a function of time is shown in Fig. 8(b). The terminal velocities are plotted in Fig. 9. Thus we have a model for which the largest particles remain aloft for a relatively short period of time while the smaller particles may remain suspended for many minutes.

A set of attenuations were computed, using the WESCOM code, as a function of frequency, elevation angle, distance from the burst and time after burst for a megaton surface burst. In Fig. 10 the attenuation is plotted as a function of time for a slant path 30° above the horizon, distance from burst of 10 km and frequencies of 10, 20, 45 and 95 GHz. It is seen that the attenuation has essentially two peaks; the first peak occurs about 35 seconds after the burst and is caused by the dust rising through the antenna beam, the broader and lower attenuation second peak is due to the settling dust passing through the beam again. As expected, dust attenuation increases significantly with frequency.

In Fig. 11 the angle dependence of the attenuation is examined for the same conditions at a frequency of 45 GHz. As expected the first peak occurs earliest and the attenuation is highest for the lowest elevation angle. Also the separation in time of the peaks decreases with increasing elevation angle.

In Fig. 12 the distance dependence of the attenuation is plotted for the same conditions for a fixed elevation angle of 30° . It is seen that the highest attenuations occur earliest for distances closest to the burst and then decrease and occur at later times as the distance from the burst is increased.

In general it is seen that high attenuations occur at all frequencies as the rising dust cloud passes through the antenna beam. For low elevation angles and distances close to the burst these attenuations may exceed 100 dB. Attenuations produced by the falling dust are significantly lower and do not generally exceed 5 dB.

5. CONCLUSIONS

Upon examining the effects of dust on slant path propagation at millimeter wavelengths it has been shown that the attenuation is heavily dependent on the maximum particle radius, the number of large particles in the distribution and the real and imaginary components of the index of refraction in the range from dry sand to clay. The attenuation is also directly proportional to the fraction of the atmosphere filled with dust. Dust attenuations, while low at frequencies below 10 GHz increase significantly at millimeter wavelengths.

For the WESCOM code, the computed attenuations behave as would be expected. Very large attenuations occur immediately after the burst due to fireball ionization and dust when the antenna beam is close to the fireball. At later times the attenuation is caused mostly by dust. The attenuation due to oxygen and water vapor is typically less than 1 dB in the window regions.

On the basis of these results it appears that if the antenna beam intersects the fireball within the first 20 seconds after the burst, then attenuations greater than 100 dB are likely, and the lower frequencies are attenuated more than the higher frequencies because the losses are due predominantly to fireball ionization. For this reason it would seem that the very early dust model is not too critical since the attenuations are always prohibitive. At times from about 20 seconds to several minutes, the period after ionization losses have essentially disappeared, but during which dust losses can be tens of dBs, the accuracy of the dust model parameters discussed above can significantly influence the results. Finally, when the dust settles, although attenuations of the order of several dB are likely, it would seem that it should be possible to model these more accurately than those at earlier times since the terminal velocities of the dust particles are known. Since only the very small particles remain suspended the size distribution is less critical and only the density and index of refraction of the dust are important.

REFERENCES

1. Mie, G., Contribution to the Optics of Suspended Media Specifically Colloidal Metal Suspensions (In German), Ann. Physik, 25, (1908) 377-445.
2. Thompson, Dust Clouds - Models and Propagation Effects, Proceedings of Submillimeter Atmospheric Propagation Applicable to Radar and Missile Systems, Redstone Arsenal, AL. TR 80-3, (1980) pp. 114-117.
3. Van De Hulst, H.C., Light Scattering by Small Particles, Wiley, NY, (1957).

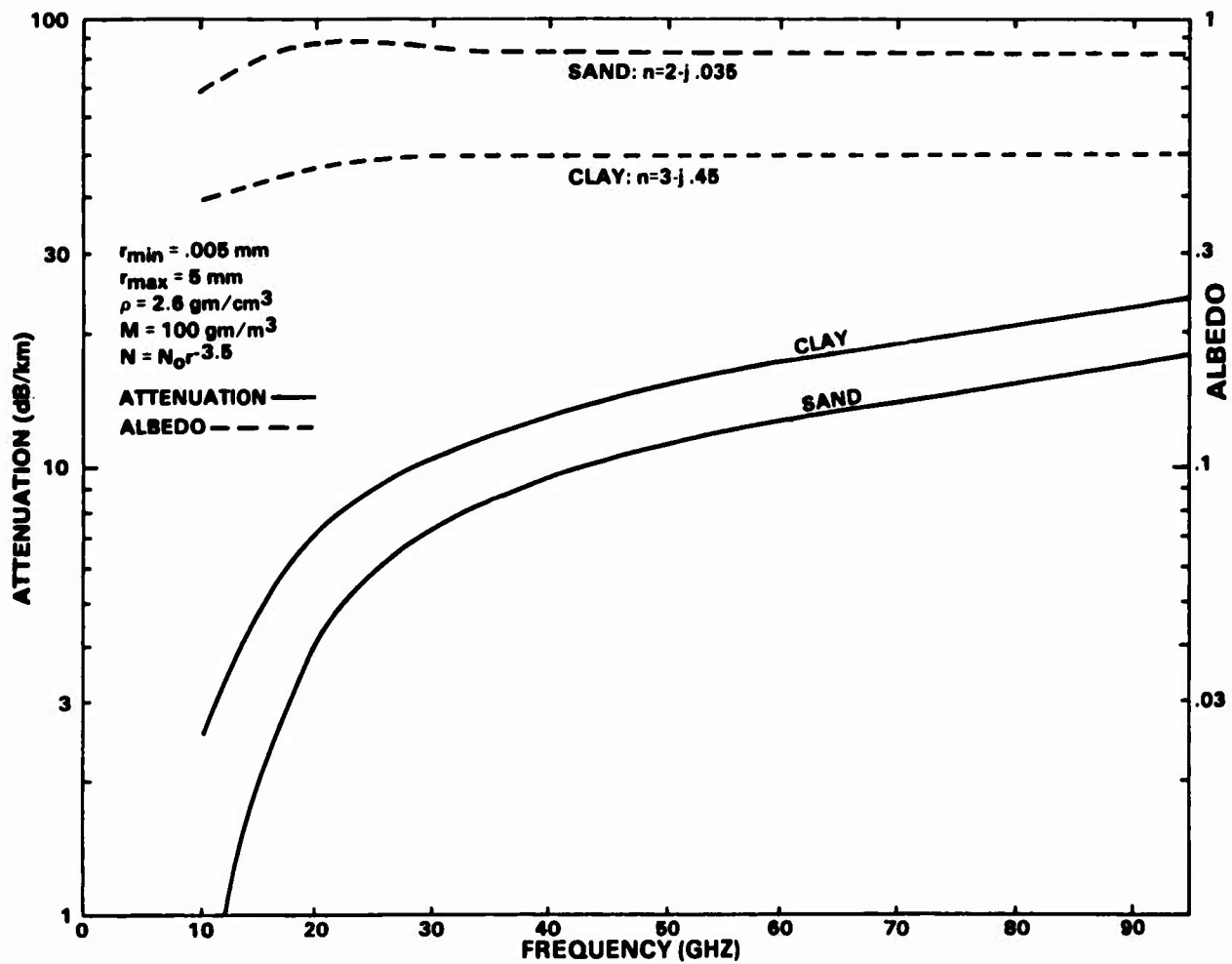


Fig. 1 Attenuation and albedo of sand and clay particles at millimeter wavelengths.

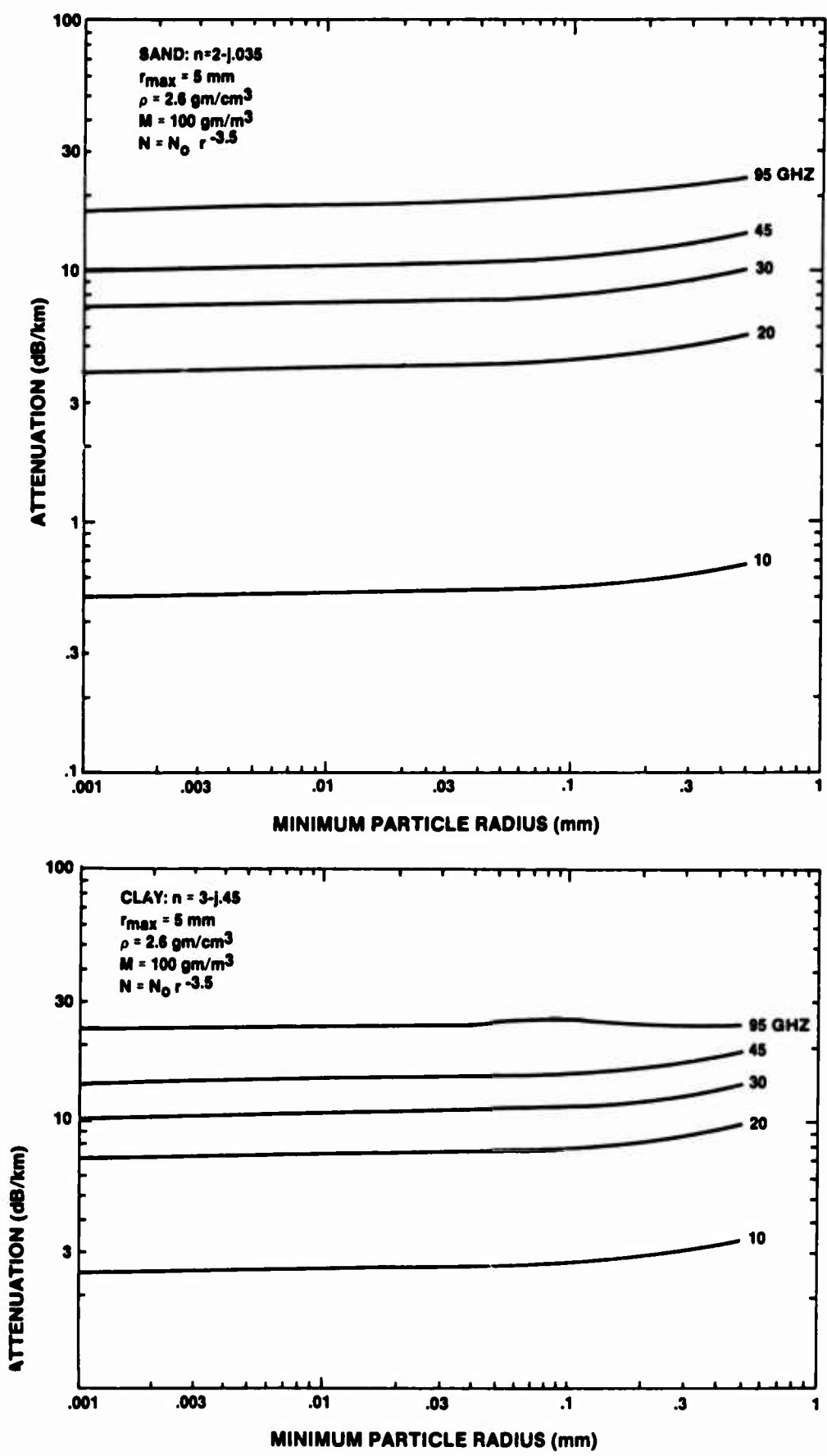


Fig. 2 Attenuation at millimeter wavelengths as a function of minimum particle radius

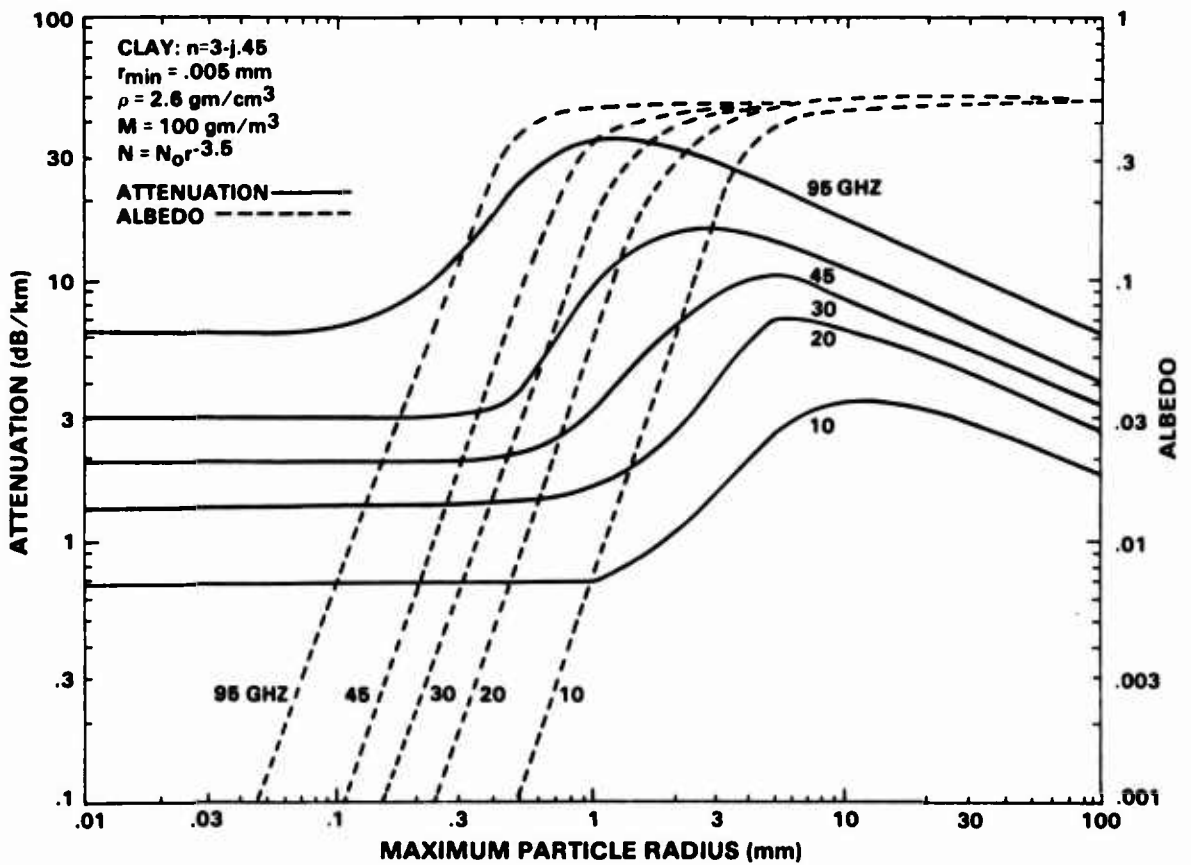
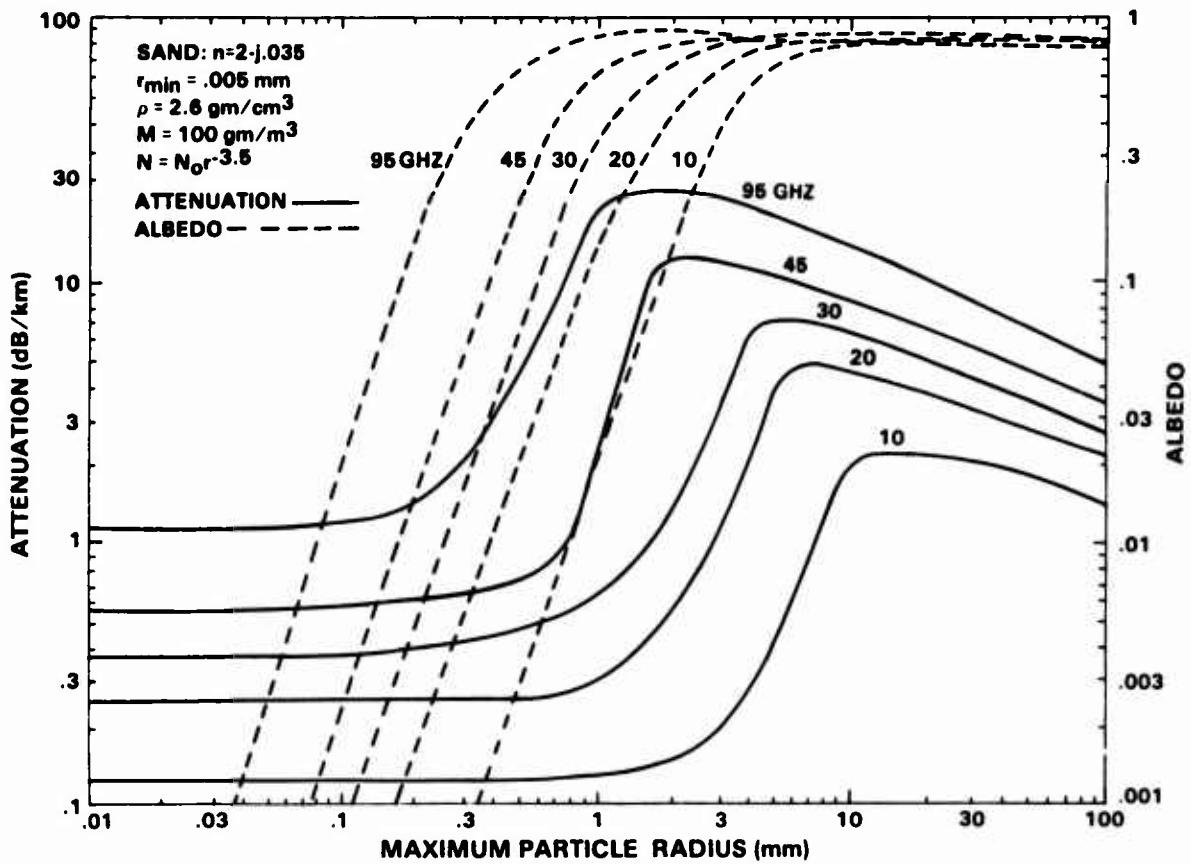


Fig. 3 Attenuation and albedo at millimeter wavelengths as a function of maximum particle radius

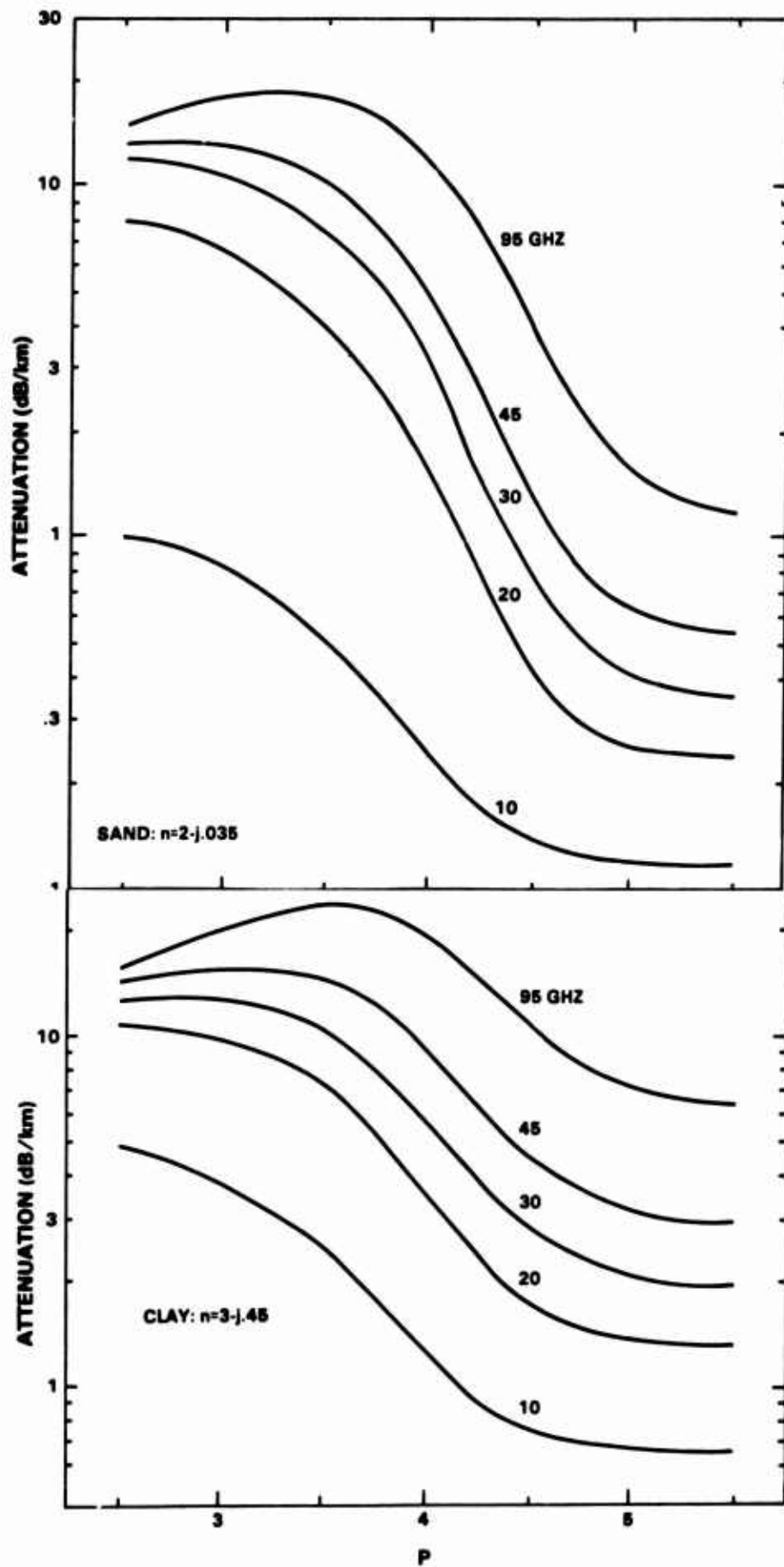


Fig. 4 Attenuation at millimeter wavelengths as a function of power law exponent

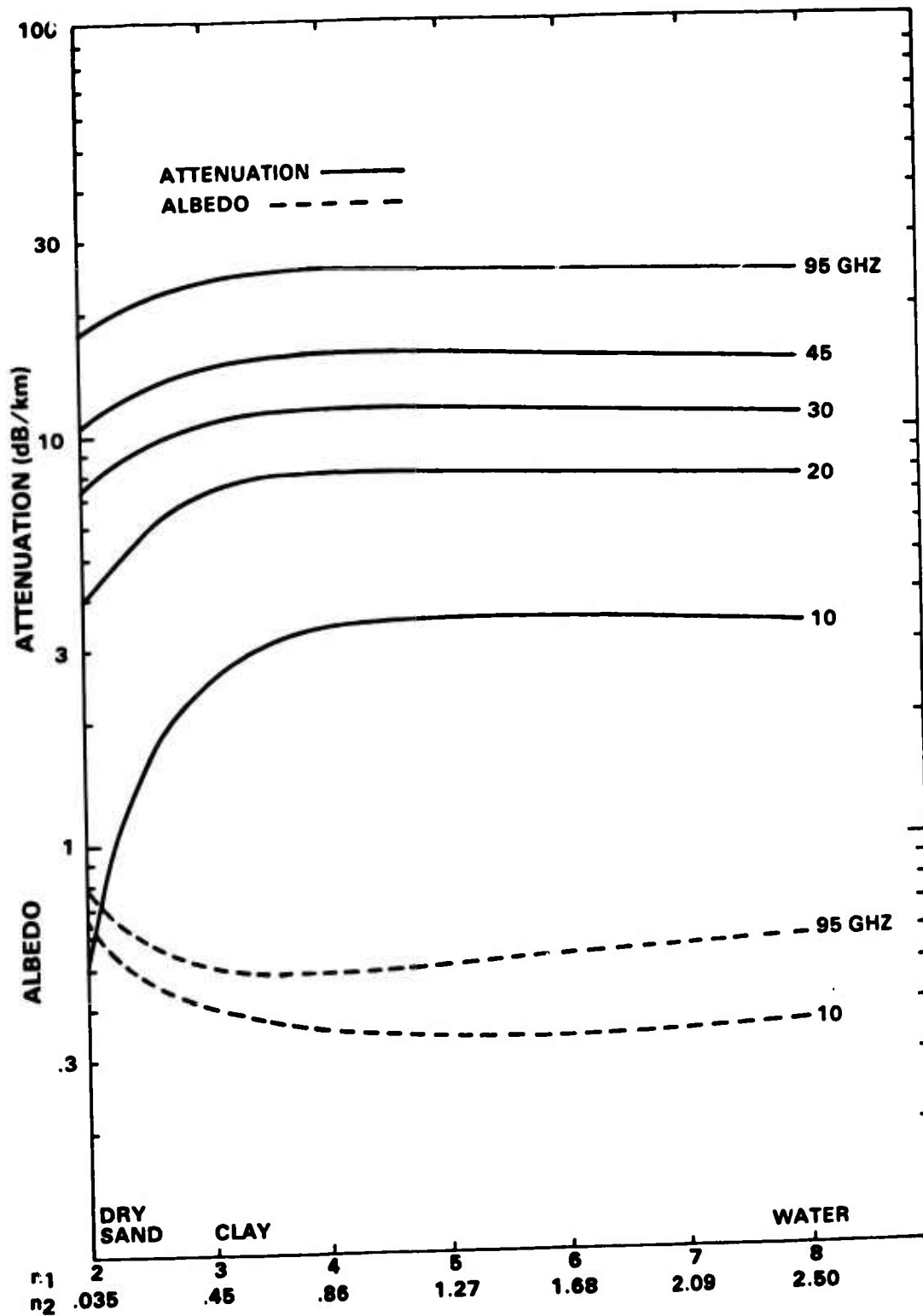


Fig. 5 Attenuation and albedo at millimeter wavelengths as a function of index of refraction.

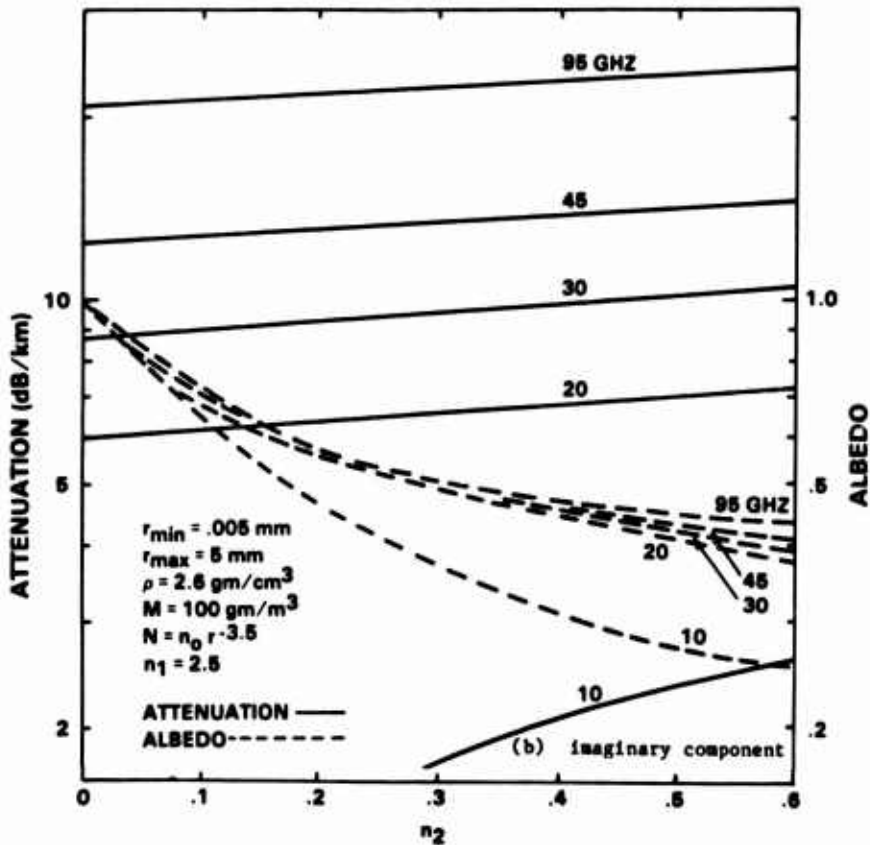
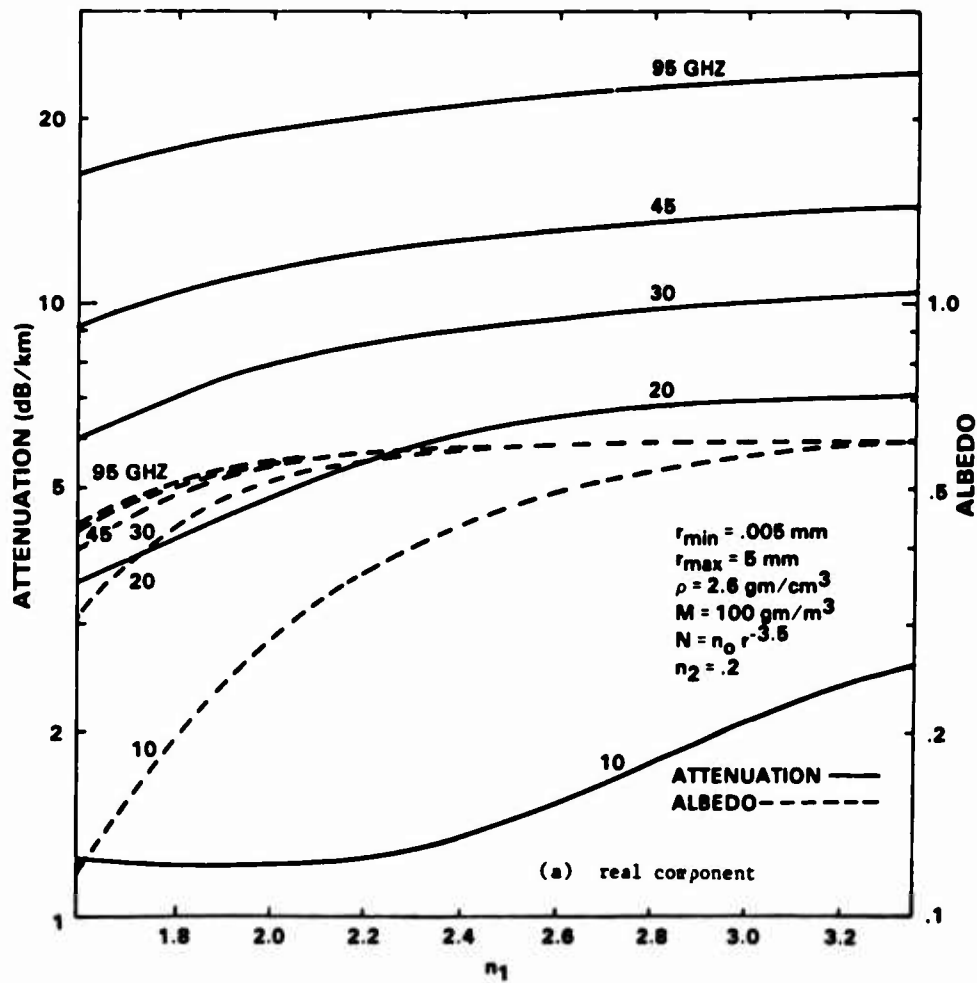


Fig. 6 Attenuation and albedo at millimeter wavelengths as a function of real and imaginary components of index of refraction.

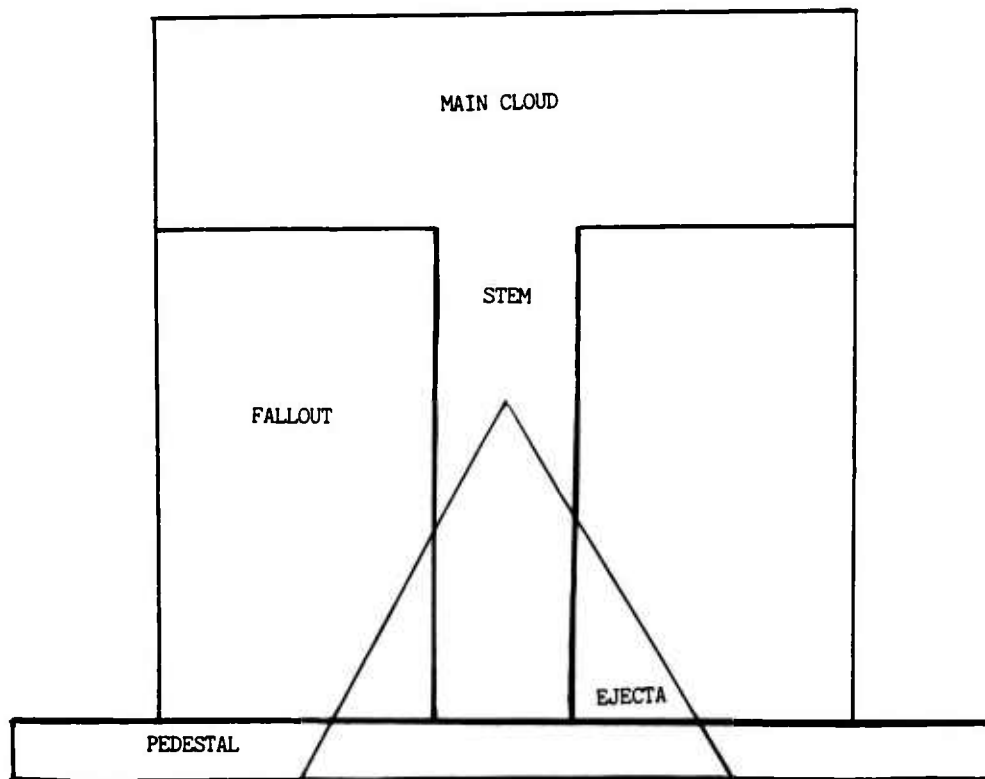
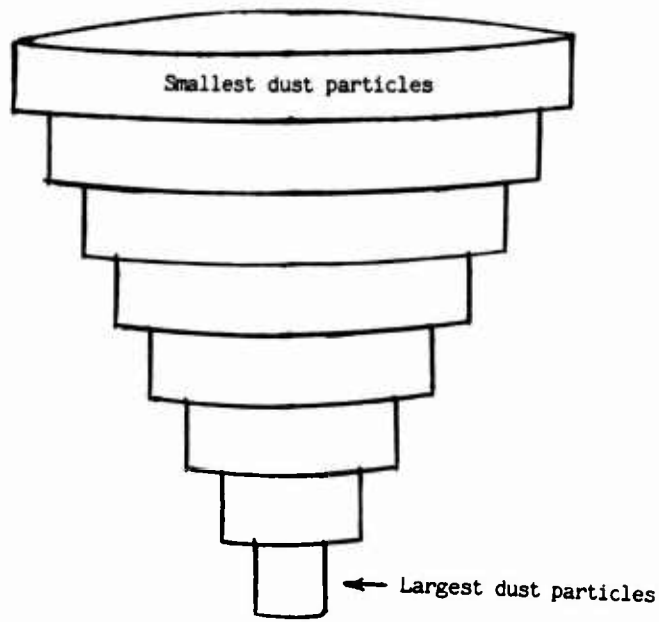
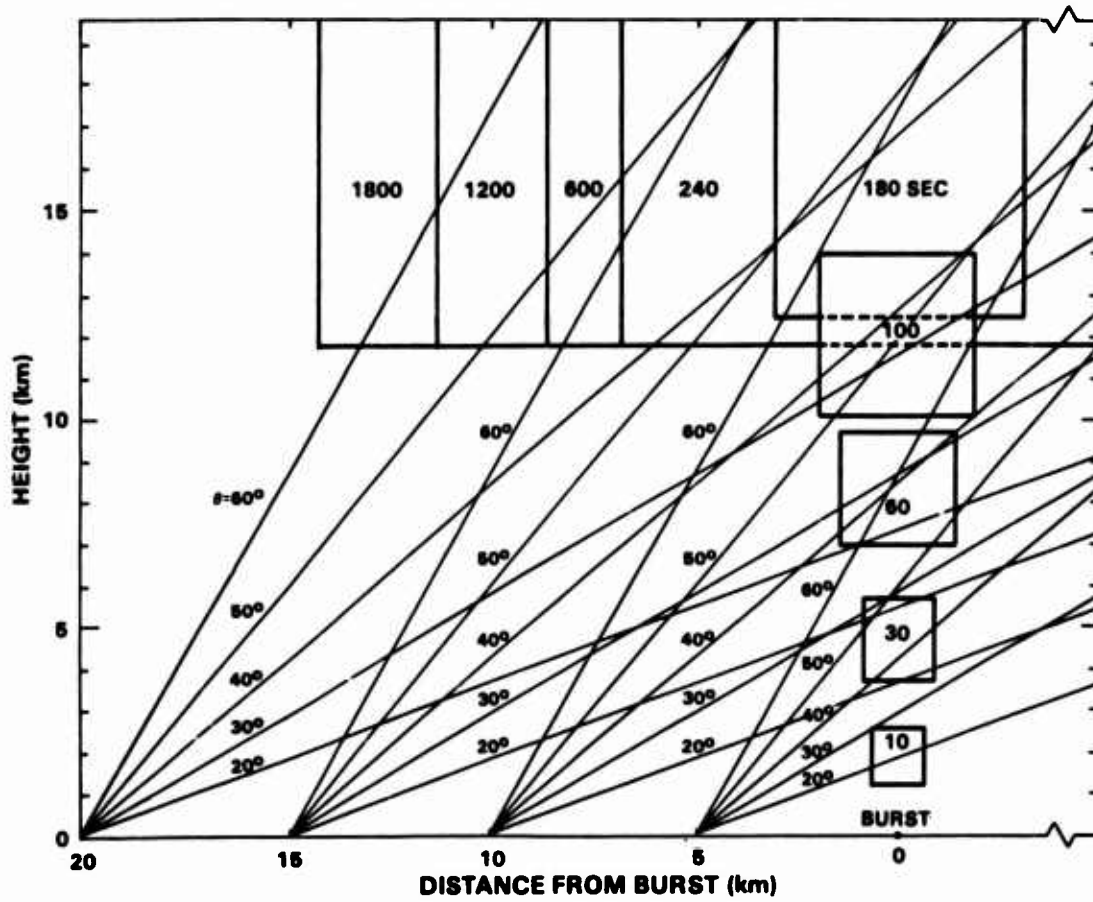


Fig. 7 Dust regions



(a) Disc-like regions within fireball



(b) Rising fireball as a function of time

Fig. 8 Dust model

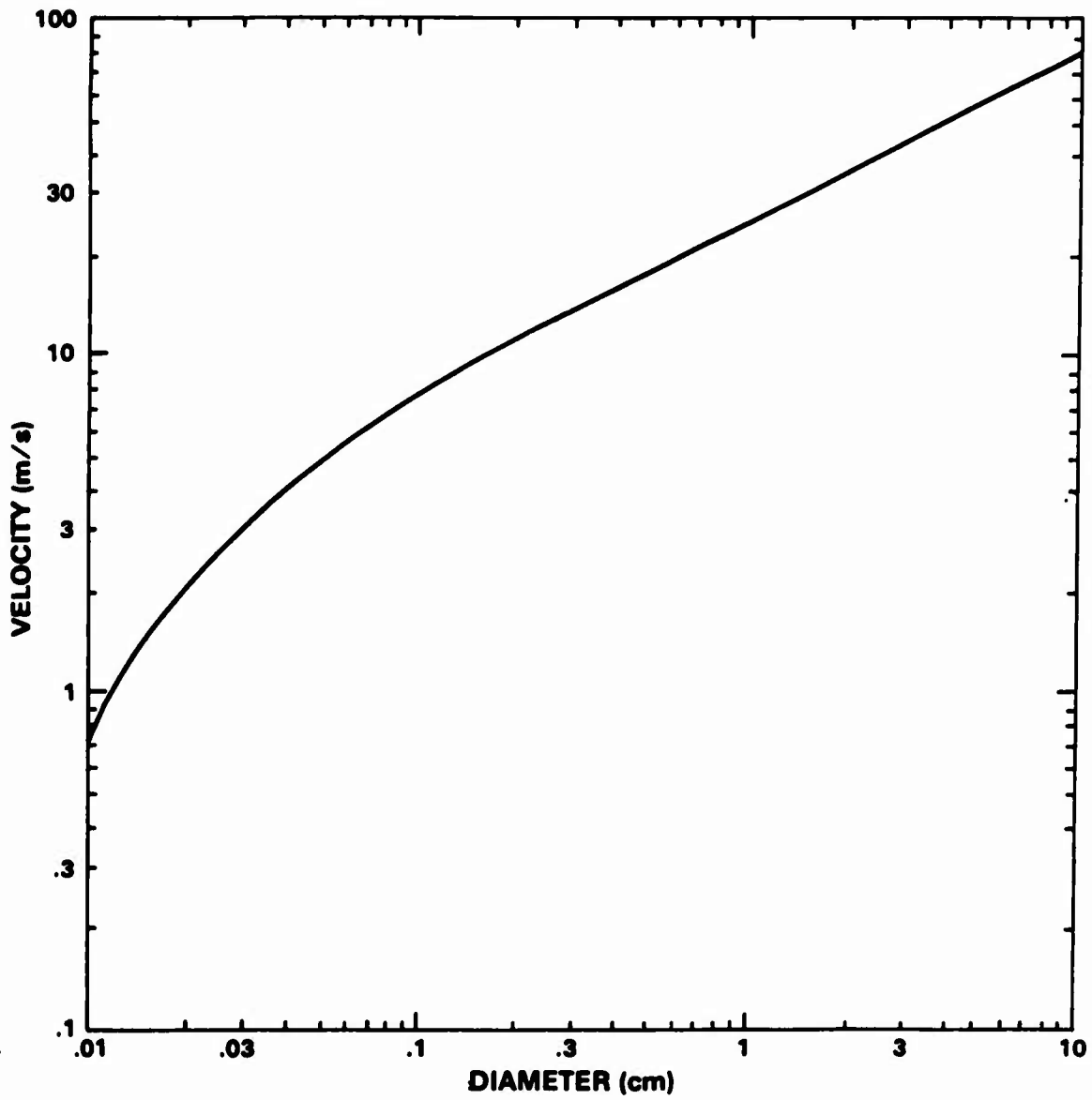


Fig. 9 Terminal velocity of dust as a function of particle radius.

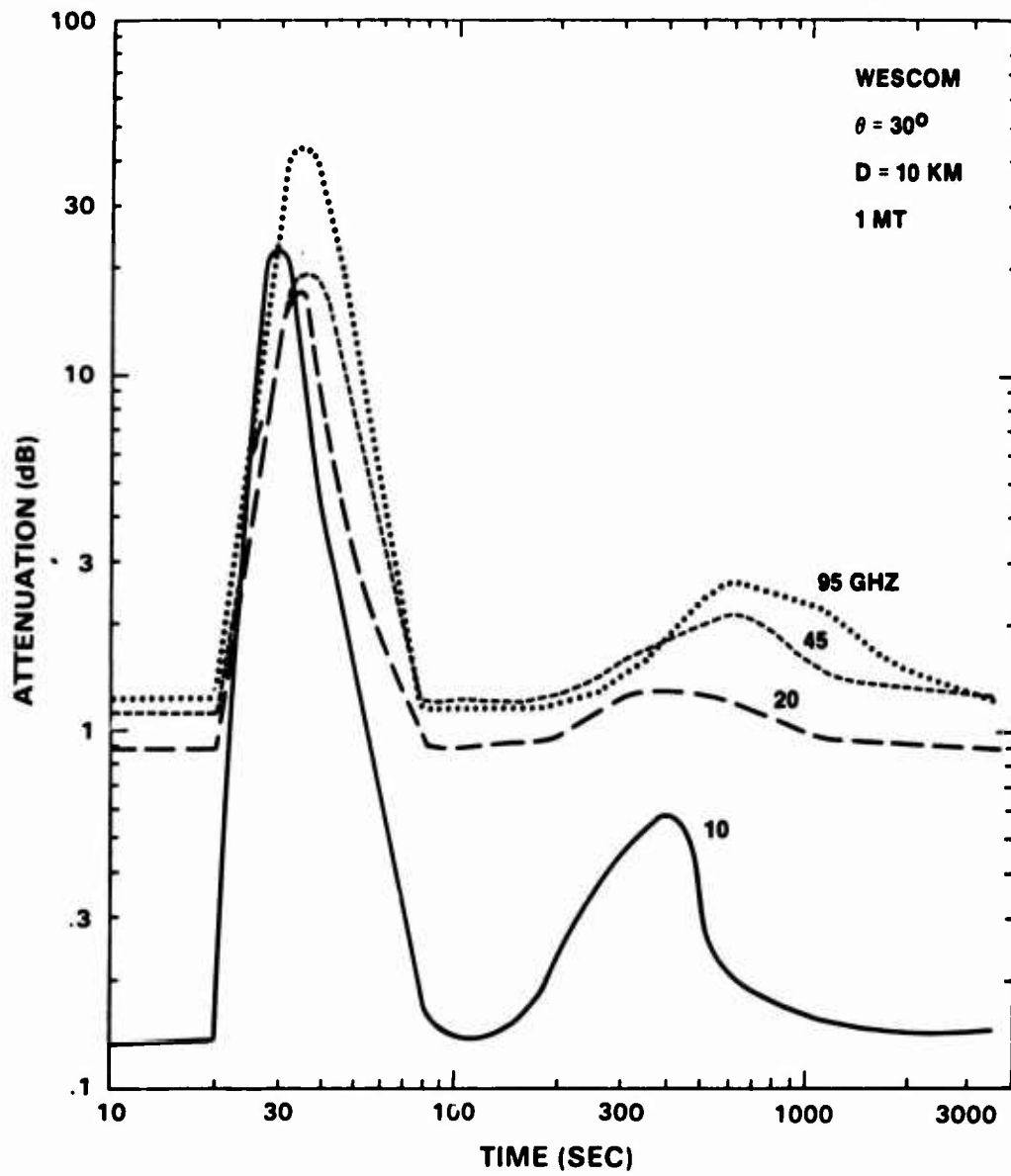


Fig. 10 Attenuation from 1 MT burst as a function of frequency.

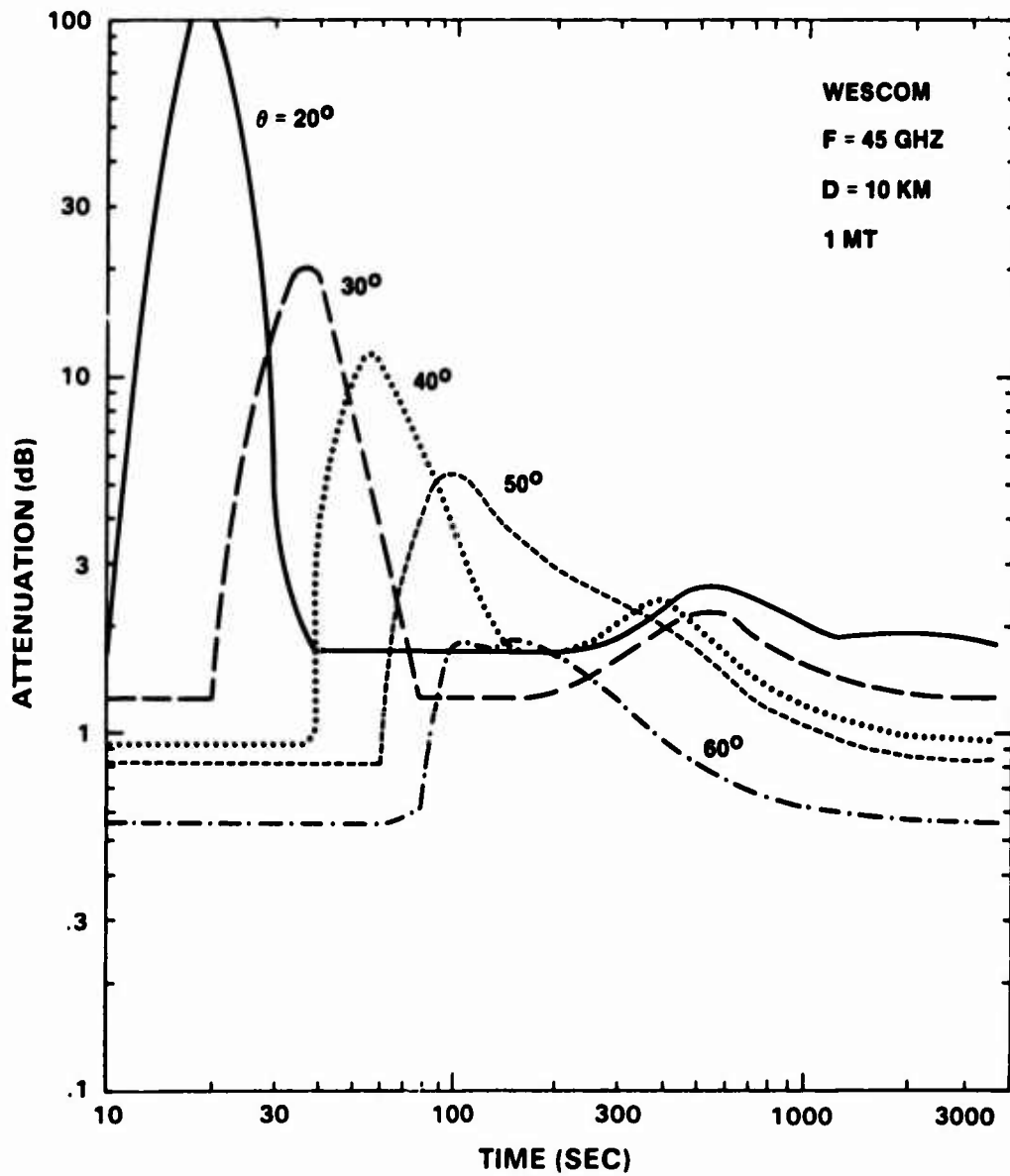


Fig. 11 Attenuation from 1 MT burst as a function of elevation angle.

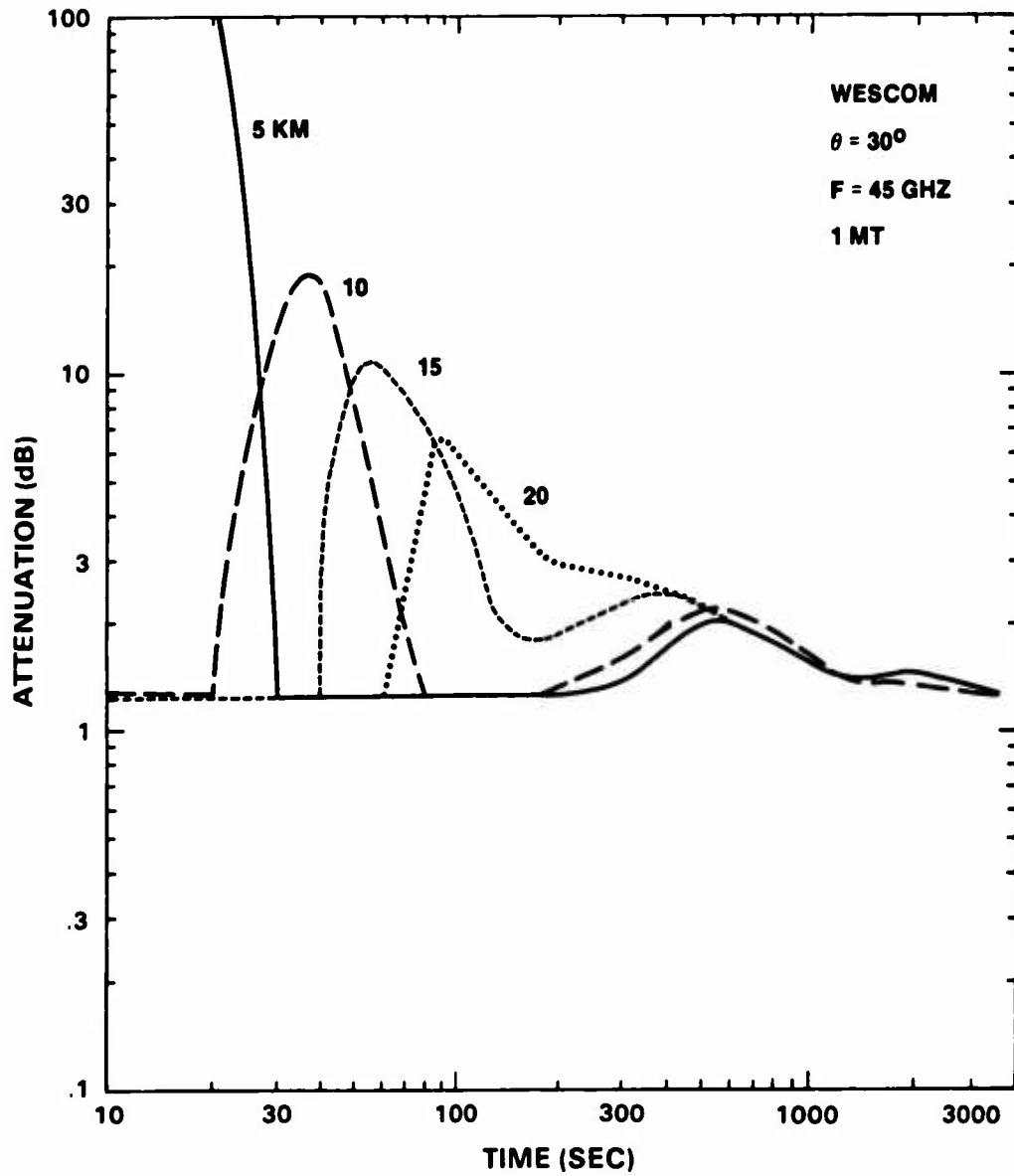


Fig. 12 Attenuation from 1 MT burst as a function of distance from burst.

DISCUSSION

I. Anderson (U.K.): Since opportunities for propagation measurements through atmospheric nuclear explosions are limited, how do you substantiate the assumptions used in your theoretical model?

E. E. Altshuler (U.S.): Measurements made with conventional explosives have been extrapolated to nuclear levels. There is however a great deal of uncertainty in the nuclear dust model. Hopefully we shall never have to verify this model.

W.G. Burrows (U.K.): While you have considered the attenuation effects of dust from a nuclear explosion in your paper, have you also considered the distortion effects (and therefore attenuation) that the central "hot column" must have on the transmitted beam? There must be a very severe change of refractive index in the region of the hot column due to the change in the gas density. For example, the "hot gas" effluent from an aircraft jet engine will completely destroy a narrow beam at mm wavelengths.

E. E. Altshuler (U.S.): The distortion effects were considered. However, the attenuation effects produced by the fireball are so severe that distortion effects are believed to be of minor importance.

M.P.M. Hall (U.K.): In addition to military interest in your subject, there is civil interest in the effects of sand and dust storms. Figure 3 in your paper shows specific attenuation in dB/km for particles up to 100 μ m radius and for an atmospheric particle density M of 100 gm/m^3 . When the radius of particles is below 0.3 μ m in natural sand and dust storms, your Figure 3 indicates that specific attenuation becomes independent of maximum particle size and scales directly with M . Could you please comment on likely values of M in these storms?

E. E. Altshuler (U.S.): Although there is only limited data on the particle size distribution of naturally occurring dust, indications are that the maximum particle sizes would be less than a few μ m. Thus the Rayleigh approximation is valid and dust attenuation is directly proportional to the mass density of dust. Attenuations for other mass densities can be estimated from Figure 3.

